How fast can we scan patients with modern (digital) PET/CT systems?

Nicolas Coudrais

UNIVERSITÉ de CAEN NORMANDIE

UFR SANTÉ

FACULTÉ de MÉDECINE

Année 2019/2020

THÈSE POUR L'OBTENTION

DU GRADE DE DOCTEUR EN MÉDECINE

Présentée et soutenue publiquement le : 30 juin 2020

par

M. Nicolas COUDRAIS

Né (e) le 14 avril 1992 à Maisons Laffitte (*Yvelines*)

TITRE DE LA THÈSE :

How fast can we scan patients with modern (digital) PET/CT systems?

Président : **Monsieur le Professeur Denis AGOSTINI**

Membres : Monsieur le Professeur Nicolas AIDE

Monsieur le Professeur Alain MANRIQUE

Madame le Docteur Charline LASNON

Directeur de thèse : ***Pr Nicolas AIDE***

UNIVERSITÉ DE CAEN · NORMANDIE

UFR SANTÉ - FACULTE DE MEDECINE

Année Universitaire 2019/2020

Doyen
Professeur Emmanuel TOUZÉ

Assesseurs
Professeur Paul MILLIEZ (pédagogie)
Professeur Guy LAUNOY (recherche)
Professeur Sonia DOLLFUS & Professeur Evelyne EMERY (3ème cycle)

Directrice administrative
Madame Sarah CHEMTOB

PROFESSEURS DES UNIVERSITÉS - PRATICIENS HOSPITALIERS

M.	**AGOSTINI Denis**	Biophysique et médecine nucléaire
M.	**AIDE Nicolas**	Biophysique et médecine nucléaire
M.	**ALLOUCHE Stéphane**	Biochimie et biologie moléculaire
M.	**ALVES Arnaud**	Chirurgie digestive
M.	**AOUBA Achille**	Médecine interne
M.	**BABIN Emmanuel**	Oto-Rhino-Laryngologie
M.	**BÉNATEAU Hervé**	Chirurgie maxillo-faciale et stomatologie
M.	**BENOIST Guillaume**	Gynécologie - Obstétrique
M.	**BERGER Ludovic**	Chirurgie vasculaire
M.	**BERGOT Emmanuel**	Pneumologie
M.	**BIBEAU Frédéric**	Anatomie et cytologie pathologique
Mme	**BRAZO Perrine**	Psychiatrie d'adultes
M.	**BROUARD Jacques**	Pédiatrie
M.	**BUSTANY Pierre**	Pharmacologie
Mme	**CHAPON Françoise**	Histologie, Embryologie
Mme	**CLIN-GODARD Bénédicte**	Médecine et santé au travail
M.	**DAMAJ Ghandi Laurent**	Hématologie
M.	**DAO Manh Thông**	Hépatologie-Gastro-Entérologie
M.	**DAMAJ Ghandi Laurent**	Hématologie
M.	**DEFER Gilles**	Neurologie
M.	**DELAMILLIEURE Pascal**	Psychiatrie d'adultes
M.	**DENISE Pierre**	Physiologie
Mme	**DOLLFUS Sonia**	Psychiatrie d'adultes
M.	**DREYFUS Michel**	Gynécologie - Obstétrique
M.	**DU CHEYRON Damien**	Réanimation médicale

Mme	**ÉMERY Evelyne**	Neurochirurgie
M.	**ESMAIL-BEYGUI Farzin**	Cardiologie
Mme	**FAUVET Raffaèle**	Gynécologie – Obstétrique
M.	**FISCHER Marc-Olivier**	Anesthésiologie et réanimation
M.	**GÉRARD Jean-Louis**	Anesthésiologie et réanimation
M.	**GUILLOIS Bernard**	Pédiatrie
Mme	**GUITTET-BAUD Lydia**	Epidémiologie, économie de la santé et prévention
M.	**HABRAND Jean-Louis**	Cancérologie option Radiothérapie
M.	**HAMON Martial**	Cardiologie
Mme	**HAMON Michèle**	Radiologie et imagerie médicale
M.	**HANOUZ Jean-Luc**	Anesthésie et réa. médecine péri-opératoire
M.	**HULET Christophe**	Chirurgie orthopédique et traumatologique
M.	**ICARD Philippe**	Chirurgie thoracique et cardio-vasculaire
M.	**JOIN-LAMBERT Olivier**	Bactériologie - Virologie
Mme	**JOLY-LOBBEDEZ Florence**	Cancérologie
M.	**JOUBERT Michael**	Endocrinologie
M.	**LAUNOY Guy**	Epidémiologie, économie de la santé et prévention
M.	**LE HELLO Simon**	Bactériologie-Virologie
Mme	**LE MAUFF Brigitte**	Immunologie
M.	**LOBBEDEZ Thierry**	Néphrologie
M.	**LUBRANO Jean**	Chirurgie viscérale et digestive
M.	**MAHE Marc-André**	Cancérologie
M.	**MANRIQUE Alain**	Biophysique et médecine nucléaire
M.	**MARCÉLLI Christian**	Rhumatologie
M.	**MARTINAUD Olivier**	Neurologie
M.	**MAUREL Jean**	Chirurgie générale
M.	**MILLIEZ Paul**	Cardiologie
M.	**MOREAU Sylvain**	Anatomie/Oto-Rhino-Laryngologie
M.	**MOUTEL Grégoire**	Médecine légale et droit de la santé
M.	**NORMAND Hervé**	Physiologie
M.	**PARIENTI Jean-Jacques**	Biostatistiques, info. médicale et tech. de communication
M.	**PELAGE Jean-Pierre**	Radiologie et imagerie médicale
Mme	**PIQUET Marie-Astrid**	Nutrition
M.	**QUINTYN Jean-Claude**	Ophtalmologie
Mme	**RAT Anne-Christine**	Rhumatologie
M.	**RAVASSE Philippe**	Chirurgie infantile
M.	**REPESSE Yohann**	Hématologie

M.	**REZNIK Yves**	Endocrinologie
M.	**ROD Julien**	Chirurgie infantile
M.	**ROUPIE Eric**	Médecine d'urgence
Mme	**THARIAT Juliette**	Radiothérapie
M.	**TILLOU Xavier**	Urologie
M.	**TOUZÉ Emmanuel**	Neurologie
M.	**TROUSSARD Xavier**	Hématologie
Mme	**VABRET Astrid**	Bactériologie - Virologie
M.	**VERDON Renaud**	Maladies infectieuses
Mme	**VERNEUIL Laurence**	Dermatologie
M.	**VIVIEN Denis**	Biologie cellulaire

PROFESSEURS ASSOCIÉS DES UNIVERSITÉS A MI-TEMPS

M.	**DE LA SAYETTE Vincent**	Neurologie
Mme	**DOMPMARTIN-BLANCHÈRE Anne**	Dermatologie
M.	**GUILLAUME Cyril**	Médecine palliative
M.	**LE BAS François**	Médecine Générale
M.	**SABATIER Rémi**	Cardiologie

PRCE

Mme	**LELEU Solveig**	Anglais

PROFESSEURS EMERITES

M.	**HURAULT de LIGNY Bruno**	Néphrologie
Mme	**KOTTLER Marie-Laure**	Biochimie et biologie moléculaire
M.	**LE COUTOUR Xavier**	Epidémiologie, économie de la santé et prévention
M.	**LEPORRIER Michel**	Hématologie
M.	**VIADER Fausto**	Neurologie

UNIVERSITÉ DE CAEN · NORMANDIE

UFR SANTÉ - FACULTE DE MEDECINE

Année Universitaire 2019/2020

Doyen
Professeur Emmanuel TOUZÉ

Assesseurs
Professeur Paul MILLIEZ (pédagogie)
Professeur Guy LAUNOY (recherche)
Professeur Sonia DOLLFUS & Professeur Evelyne EMERY (3ème cycle)

Directrice administrative
Madame Sarah CHEMTOB

MAITRES DE CONFERENCES DES UNIVERSITÉS - PRATICIENS HOSPITALIERS

M.	**ALEXANDRE Joachim**	Pharmacologie clinique
Mme	**BENHAÏM Annie**	Biologie cellulaire
M.	**BESNARD Stéphane**	Physiologie
Mme	**BONHOMME Julie**	Parasitologie et mycologie
M.	**BOUVIER Nicolas**	Néphrologie
M.	**COULBAULT Laurent**	Biochimie et Biologie moléculaire
M.	**CREVEUIL Christian**	Biostatistiques, info. médicale et tech. de communication
M.	**DE BOYSSON Hubert**	Médecine interne
Mme	**DINA Julia**	Bactériologie - Virologie
Mme	**DUPONT Claire**	Pédiatrie
M.	**ÉTARD Olivier**	Physiologie
M.	**GABEREL Thomas**	Neurochirurgie
M.	**GRUCHY Nicolas**	Génétique
M.	**GUÉNOLÉ Fabian**	Pédopsychiatrie
M.	**HITIER Martin**	Anatomie - ORL Chirurgie Cervico-faciale
M.	**ISNARD Christophe**	Bactériologie Virologie
M.	**JUSTET Aurélien**	Pneumologie
Mme	**KRIEGER Sophie**	Pharmacie
M.	**LEGALLOIS Damien**	Cardiologie
Mme	**LELONG-BOULOUARD Véronique**	Pharmacologie fondamentale
Mme	**LEVALLET Guénaëlle**	Cytologie et Histologie
M.	**MITTRE Hervé**	Biologie cellulaire
M.	**SESBOÜÉ Bruno**	Physiologie
M.	**TOUTIRAIS Olivier**	Immunologie
M.	**VEYSSIERE Alexis**	Chirurgie maxillo-faciale et stomatologie

MAITRES DE CONFERENCES ASSOCIÉS DES UNIVERSITÉS A MI-TEMPS

Mme	**ABBATE-LERAY Pascale**	Médecine générale
M.	**COUETTE Pierre-André**	Médecine générale
Mme	**NOEL DE JAEGHER Sophie**	Médecine générale
M.	**PITHON Anni**	Médecine générale
M.	**SAINMONT Nicolas**	Médecine générale
Mme	**SCHONBRODT Laure**	Médecine générale

MAITRES DE CONFERENCES EMERITES

Mme	**DEBRUYNE Danièle**	Pharmacologie fondamentale
Mme	**DERLON-BOREL Annie**	Hématologie
Mme	**LEPORRIER Nathalie**	Génétique

Remerciements

À Monsieur le Professeur Denis AGOSTINI, de me faire l'honneur de présider ce jury et de juger mon travail. Veuillez trouver ici toute ma reconnaissance et l'expression de mon profond respect.

À Monsieur le Professeur Nicolas AIDE, pour avoir accepté de diriger mon travail de thèse, pour m'avoir transmis son savoir et encadré durant ces années d'internat. Enfin, merci pour m'avoir fait sourire si souvent.

À Madame le Docteur Charline LASNON, de s'être rendue disponible, merci pour son implication dans ce travail même si nous n'avons pas partagé de semestre ensemble, c'était un plaisir.

À Monsieur le Professeur Alain MANRIQUE, d'avoir accepté de juger mon travail et surtout pour l'enseignement et la bonne humeur apportée durant ma formation. Merci de m'avoir permis de participer au congrès de Barcelone, une étape stressante mais une très bonne expérience.

À toutes les équipes médicales et paramédicales du service de médecine nucléaire du CHU de Caen ainsi que du Centre François Baclesse, du service de cardiologie du Centre Hospitalier Mémorial de Saint-Lô, et des services de Radiologie et Radiothérapie du Centre François Baclesse.

À l'ensemble de mes co-internes de médecine nucléaire et d'autres spécialités, rencontrés lors de mes différents stages.

À Claire, ma femme, pour le meilleur (et puis c'est tout), pour me soutenir, pour m'épauler, pour ton sens de l'humour, pour ta bonne humeur, pour ta générosité, pour ta délicatesse, pour tes discussions interminables, pour ta correction des fautes d'orthographe et pour un millier d'autres choses encore, et ce depuis près de 10 ans ! Tu m'as fait grandir et je suis grâce à toi quelqu'un de meilleur (enfin je l'espère).

À mon frère, Antoine, qui me permet d'être si joyeux au quotidien tant il déborde de bonne humeur. Ne change rien à ta façon d'être, continue de sourire, aie confiance en toi, tu es unique, tu es le meilleur (sauf au golf). Merci également à Louise qui prend soin de lui ; hâte de suivre vos prochaines aventures !

À mes parents, qui m'ont toujours soutenu dans mes choix et inculqué les valeurs de travail et de rigueur qui m'ont permis d'arriver là où je suis. Merci de m'avoir guidé et aidé à réussir les projets entrepris. Merci à vous d'être restés proches malgré la distance.

À mes grands-parents, qui se sont dévoués pour mon frère et moi, qui ont toujours fait en sorte que l'on ne manque de rien et avec qui j'ai, pour chacun, un immense respect et des souvenirs plein la tête. Et bien sûr, à grand père, j'espère qu'où que tu sois, tu es fier de nous.

À mes beaux-parents, Catherine et Philippe, pour l'échange de nos expériences, et pour m'avoir permis de partager de bons moments en famille, à Compiègne ou à Cancale !

À Néné et Mamadou, qui m'ont toujours fait rire, que ce soit à la plage ou sur des skis, et qui m'ont permis d'élargir mes centres d'intérêt (halte à la médecine) !

À mes amis Amiénois, Florent, Camille, Arvind et Roman qui ont partagé avec moi ces 6 années d'externat (au moins) et qui continuent d'être une source de joie au quotidien malgré la distance. Venez en Normandie, on est bien.

À mes amis Caennais, François, Valentin, Manon, Émilie ... avec qui j'ai partagé de bons moments et déjà créé de nombreux souvenirs ! Une belle équipe composée d'une moitié de sportifs et d'une moitié de fêtards, à vous de choisir.

À toutes les personnes que je n'ai pas citées mais qui ont contribué d'une manière ou d'une autre à faire de moi la personne que je suis aujourd'hui.

Abréviations

^{18}F-FDG: 18 Fluor – FluoroDesoxyGlucose

CoV: coefficient of variation

EANM: European association of nuclear medicine

FOV: field of view

KBq/cc: Kilo Becquerel/centimètre cube

Kcps: Kilo coups

MBq: Mega Becquerel

Min: minute

MIP: maximum intensity projection

NECR: noise equivalent count rate

PERCIST: PET evaluation response criteria in solid tumors

PET/CT: positron emission tomography / computed tomography

PSF: point spread function

SD: standard deviation

SUV: standard uptake value

VOI: volume of interest

ROI: region of interest

Table des matières

Tableaux et figures

Table 1: Patient characteristics (n = 28)

Clinical indication
Dyspnea (n = 8, 28%)
Pain (n = 11, 40%)
Pediatric patients (n = 9, 32%)
Gender - (15M/13F)
Age (years)*:
Adult patients: 64.8 (12.9)
Paediatric patients: 7.5 (4.4)
Injected activity (MBq/kg)* :
Adult patients: 5 (0.7)
Paediatric patients: 5.8 (0.4)
Delay (min)*: 63 (6,67)
Glycaemia (g/l)*: 1,03 (0,27)

* Mean (SD)

Reconstructions	*Number of lesions*	*Number of sites*
1i10s20$_{sec}$*	0.78	0.72
1i10s30$_{sec}$*	0.72	0.72
2i10sPSF60$_{sec}$*	0.89	0.92

* As compared to the 2i10sPSF90 reconstruction

Table 2:

Intra-observer agreement evaluated for a PET reader who interpreted all reconstructions, starting with the supposedly worst reconstruction (in terms of noise level) and increasing the time per bed position up to the standard acquisition time.

< 0.2: poor agreement, 0.2 - 0.4: fair agreement, 0.41 - 0.6: moderate agreement, 0.61 - 0.8: good agreement, 0.8 – 1: very good

Reconstructions	*Number of lesions*	*Number of sites*
1i10s20$_{sec}$	0.64	0.68
1i10s30$_{sec}$	0.79	0.91
2i10sPSF60$_{sec}$	0.78	0.81
2i10sPSF90$_{sec}$	0.83	0.84

Table 3:

Inter-observer agreement: interpretation was compared between one reader who read the four reconstructions, and four other observers who interpreted one reconstruction each.

< 0.2: poor agreement, 0.2 - 0.4: fair agreement, 0.41 - 0.6: moderate agreement, 0.61 - 0.8: good agreement, 0.8 – 1: very good

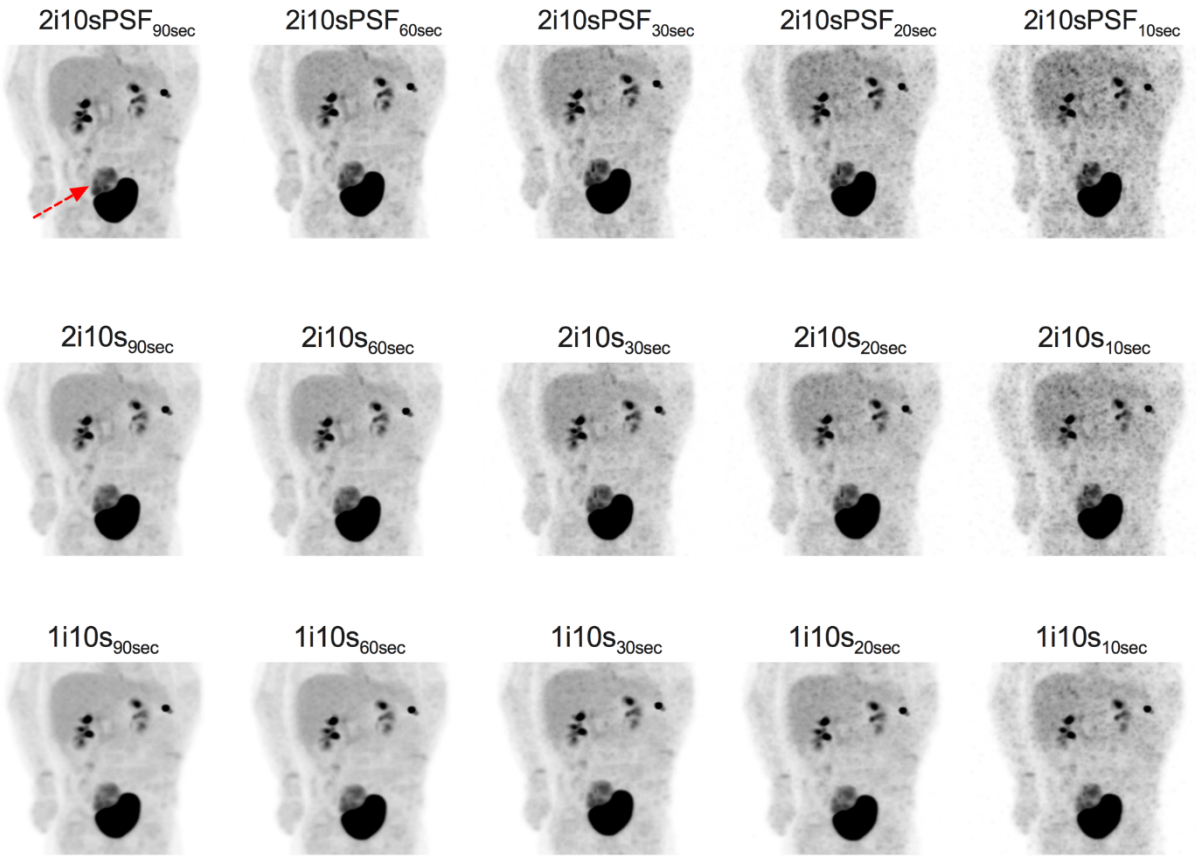

Figure 1: Illustration of the multiple reconstructions performed to simulate fast acquisition and to improve image noise in short or ultra-short simulated images. 5-year-old patient with right vesical rhabdomyosarcoma. MIP views centred on the primary tumour are shown (n=15) according to the different reconstruction times and parameters. The standard reconstruction (90s per bed position, 2 iterations 10 subsets, PSF modeling enabled).

Each reconstruction is labeled as follows: *x*i*x*s$_{x\text{sec}}$ where *x*i, *x*s and $_{x\text{sec}}$ stand for the number of iterations, the number of subsets and the time per bed position in seconds. PSF: point spread function modeling.

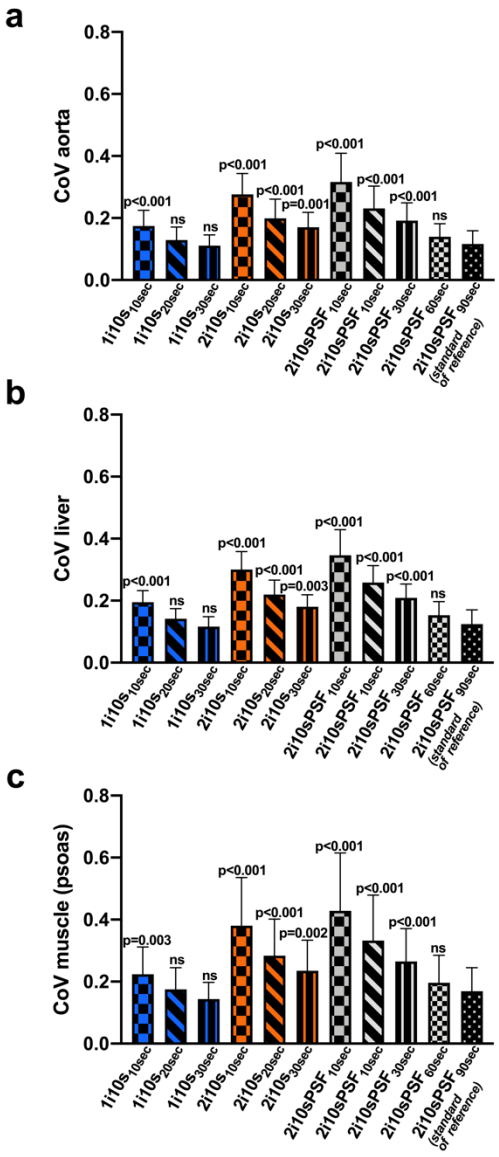

Figure 2: Noise in reference organs (a: aorta, b: liver, c: muscle) expressed as the coefficient of variation (CoV). Data are presented as mean ± standard deviation and compared to the standard reconstruction (90s per bed position, 2 iterations 10 subsets, PSF modeling enabled).

Each reconstruction is labeled as follows: *x*i*x*s$_{x\text{sec}}$ where *x*i, *x*s and $_{x\text{sec}}$ stand for the number of iterations, the number of subsets and the time per bed position in seconds. PSF: point spread function modeling.

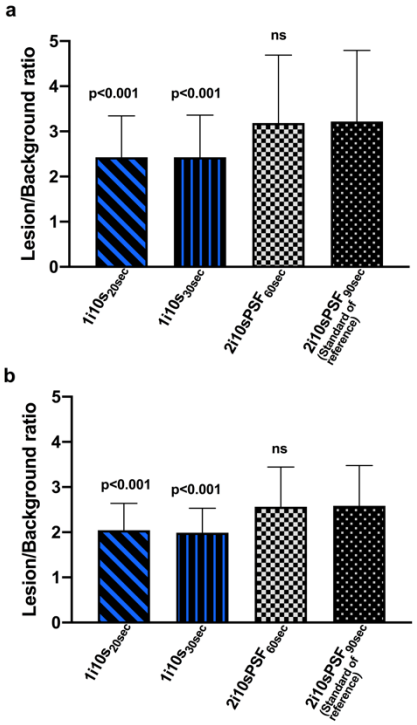

Figure 3: Lesion to background ratio using a doughnut VOI for background definition. Fast reconstructions (from 60S to 20s per bed position) were compared to the standard reconstruction (90s per bed position, 2 iterations 10 subsets, PSF modeling enabled). Analyses were performed for the more obvious lesion of each patient.

Data are shown for the most obvious (panel a) and less obvious lesion (panel b) of each PET examination.

Each reconstruction is labeled as follows: *x*i*x*s$_{x\text{sec}}$ where *x*i, *x*s and $_{x\text{sec}}$ stand for the number of iterations, the number of subsets and the time per bed position in seconds. PSF: point spread function modeling.

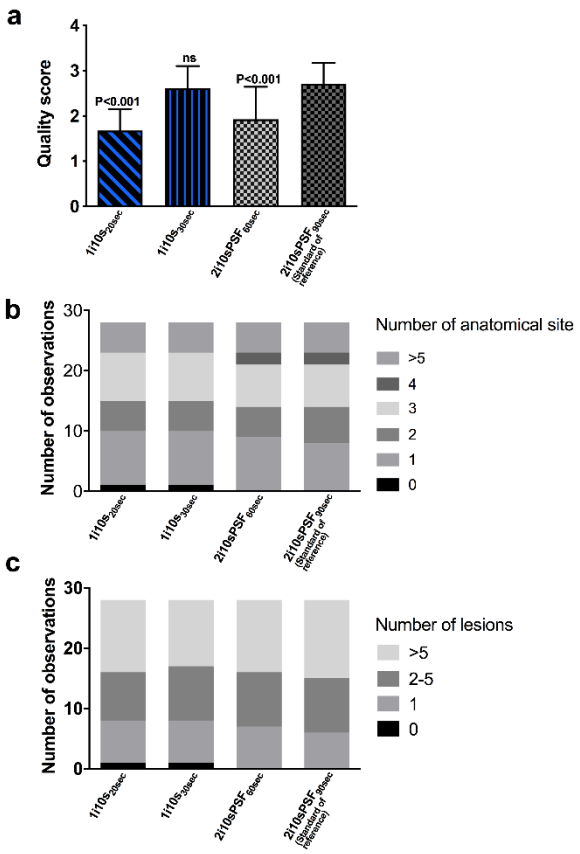

Figure 4 Comparison of the number of image quality (**a**), anatomical sites (**b**) and number of lesions (**c**): a PET reader who interpreted all reconstructions, starting with the supposedly worst reconstruction (in terms of noise level) and increasing the time per bed position up to the standard acquisition time. Each reconstruction is labeled as follows: *x*i*x*s$_{x\text{sec}}$ where *x*i, *x*s and $_{x\text{sec}}$ stand for the number of iterations, the number of subsets and the time per bed position in seconds. PSF: point spread function modeling.

The order of review was (1) 1i10s10$_{\text{sec}}$, (2) 1i10s20$_{\text{sec}}$, (3) 1i10s30$_{\text{sec}}$, (4) 2i10sPSF60$_{\text{sec}}$ and finally the standard of reference 2i10sPSF90$_{\text{sec}}$.

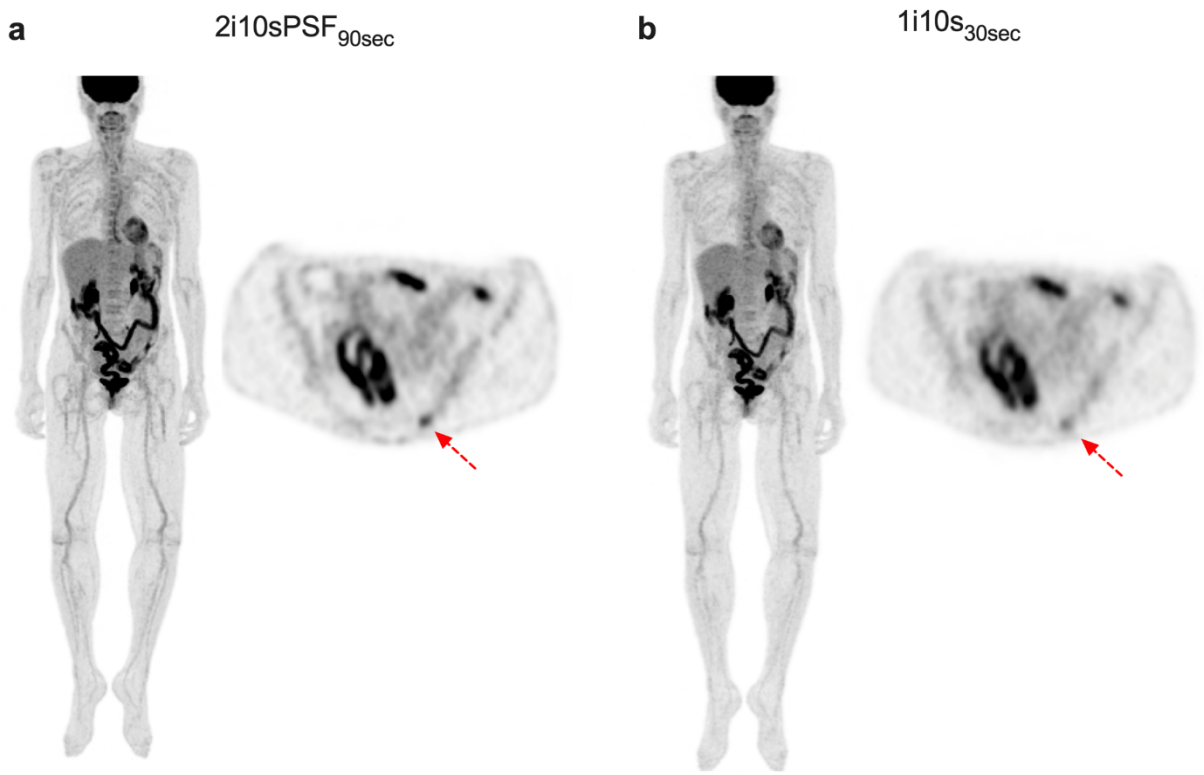

Figure 5: 63-year-old female patient with severe pain due to a myeloma recurrence. A suspicious lesion with mild uptake is seen on the posterior left iliac crest on the usual ^{18}F-FDG PET/CT acquisition (**a**, from left to right MIP view and transverse slice centred on the lesion). The lesion is still visible on simulated fast acquisition and was picked up by the blinded PET reader.

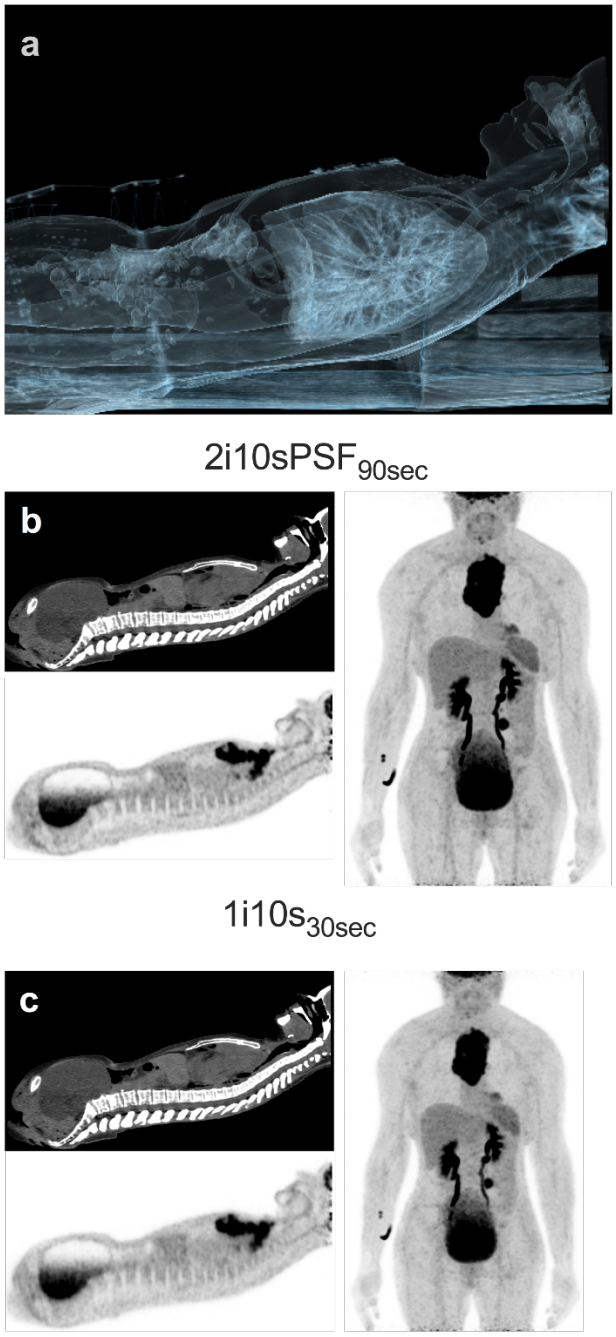

Figure 6: 62-year-old female lymphoma patient with bulky mediastinal mass and superior vena cava syndrome with significant dyspnea, who had to be scanned with several pillows (**a**). Sagittal slices are shown for CT and ^{18}F-FDG PET images with the usual parameters (**b**) or using a simulated fast acquisition with adapted reconstructed parameters (**c**).

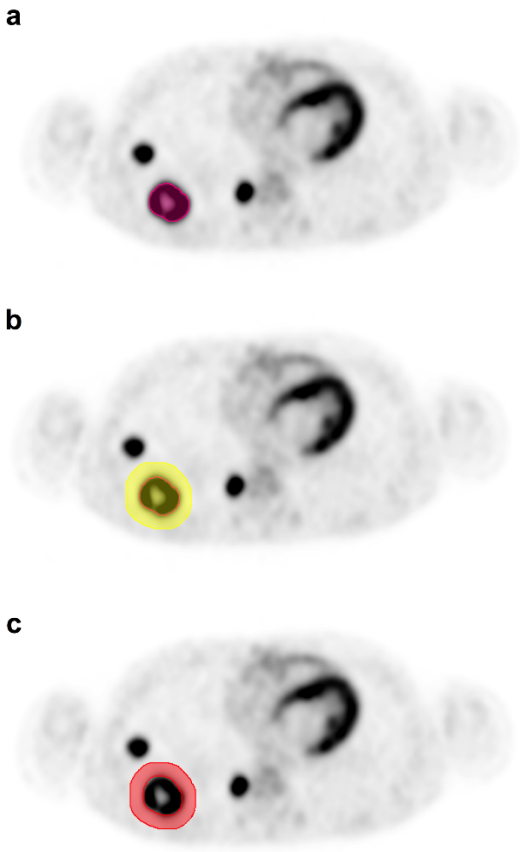

Supplemental Figure 1: Methodology for delineation of a doughnut shaped VOI surrounding the tumours' VOI used for computation of the tumour/background: **a**: gradient-based tumour VOI, **b**: 3D VOI including a 1 cm, **c**: doughnut VOI (red colour) obtained by substracting the tumour VOI to the tumour+ surrounding noise VOI

Introduction

Over the last decade, Positron emission tomography (PET) has been marked by technological involvements, including improved reconstruction algorithms and hardware evolutions [1], the most recent one being digital PET that is now available from the major PET vendors [2-6]. Fully digital PET cameras, such as the Vereos system (Philips Heathcare®, Ohio, US), feature small digital silicon photomultipliers instead of much larger photomultiplier tubes, providing true digital photon counting with 1-to-1 crystal coupling. The properties of digital systems, in particular the enhancement in the time-of-flight capabilities, have been shown to improve signal-to-noise ratio and ultimately image contrast and lesion detectability compared to analog PET [3, 7, 8]. From a daily routine perspective, these PET advancements are usually used to decrease injected activity and reduce acquisition time, the decrease in the injected activity being made with the aim of reducing radiation exposure but also for obvious economic reasons. However, evaluation of the physics performance of modern PET system with regards to noise equivalent count rate curves (NECR), which account for useful information (true coincidences) and events creating noise (random and scattered coincidences), show that recent PET scanners could handle high activity in the FOV without compromising image quality (i.e noise level).

An issue faced by PET unit teams is the management of bedridden patients experiencing pain or dyspnea. Also challenging is the scan of uncompliant pediatric patients when premedication is not efficient or feasible. Positioning of the patient on the table and PET acquisition being the bottleneck of the total scan time, the fastest PET acquisition would be very useful in all of these situations, provided the diagnostic performances are maintained.

The aim of this study was to seek the minimal duration per bed position being feasible with a recent PET system without compromising image quality and tumour or other target detection in patients for whom fast or even ultra-fast PET imaging may be useful. We focused on cancer patients with

dyspnea or in pain, as well as paediatric patients in whom recommendation for injected activity (PEDdose: https://www.eanm.org/publications/dosage-calculator/) lead to activity per unit of weight higher than those used in adult.

The minimal time per bed position was investigated by reconstructing list mode data with decreasing time down to 10 s per bed position. We also evaluated whether modifications had to be made regarding reconstruction parameters when using ultra-fast imaging (i.e in images acquired with less than 60 seconds per bed position), in order to maintain an acceptable noise level. A comprehensive evaluation of the impact of reducing acquisition time was performed on simulated data, including image quality, lesion detectability as well as inter- and intra-observer agreement.

Materials and methods

Patients' selection

From January 2018 to September 2018, patients experiencing pain or dyspnea, in whom a standard ^{18}F-FDG PET scan duration (around 20 min) was deemed to be infeasible, received a higher injected activity (arbitrary set to 5 MBq/Kg) and underwent a faster scan, as described below in the materials and methods section. Also included in this series were pediatric patients in whom the injected activity, according to the EANM guidelines (using the PETdose recommendations), usually leads to an injected activity around 5-6 Mbq/kg, which is almost twice the injected activity per unit weight in adults at our PET centre. This study was part of the NUMANATEP project, meant to evaluate digital PET systems at our institution, which was approved by the regional Ethics Committee (registration number: CERES 27669) and authorization to use additional reconstructions for research purpose was sought from every patient. Anonymised data were collected and used *as per* the European mutually agreed General Data Protection Regulation (GDPR) with the French committee on data privacy registration number CNIL 2204611 v 0.

PET/CT acquisition and reconstruction parameters

The ^{18}F-FDG usual injected activity was increased from 3 MBq/kg to 5 MBq/kg in adult patients and the acquisition time was decreased from 2 min to 1.5 min. Pediatric patients' activities were computed using the EANM PEDdose application) and these patients were also scanned at 1.5 min per bed position.

Data were acquired in list mode on a Vereos digital PET/CT system. At our centre, the standard reconstruction is as follows: 2 iterations, 20 subsets (2i20s), point spread function modelling and time-of-flight enabled, no post filtering and voxel size of 2mm^3. In addition, frames of 60s, 30s, 20s and 10s per bed position were reconstructed with the same parameters. Given that an increase in the noise level was expected for reconstructions shorter than 60s per bed position, we also

reconstructed 30, 20 and 10s per bed simulated acquisitions with (i) the same number of iterations but with PSF modeling disabled and (ii) a two-fold decrease in the number of iterations ($1i10_{sec}$) and PSF disabled. Therefore, a total of 15 reconstructions per patient were studied (Figure 1). Within this complete manuscript, the reconstructions are defined and labeled as follows: *x*i*x*s$_{x\text{Sec}}$ where *x*i, *x*s and $_{x\text{sec}}$ stand for the number of iterations, the number of subsets and the time per bed position in seconds. PSF: point spread function modeling.

Evaluation of noise and tumour/local background when decreasing the acquisition time

Images were analyzed using the MIM software. For all analysis, region of interest (ROI) and volume of interest (VOI) were drawn by one PET reader, using a gradient-based contouring method (PET edge) on images obtained with the standard reconstruction and then copied and pasted to the ten other set of images to avoid any intra-observer variability.

Noise was evaluated in large reference organs and in the vascular background as follows:

- Liver: a 3 cm diameter VOI centred on the right liver lobe
- Aorta: a 1.5 cm VOI centre on the descending aorta
- Muscles: a 1.5 cm diameter VOI placed on the right ilio-psoas muscle at the level of the 4th lumbar vertebra

In order to assess the potential lesion detectability as a function of lesion/surrounding background visual ratio, a doughnut shaped VOI surrounding the tumours' VOI was used and tumour/background ratios were computed using the SUV_{mean} values within the tumours and doughnut VOIs (supplemental figure 1). As most of included patients had multiple lesions, we focused on the most obvious and less obvious lesions on the standard reconstruction.

Comparison of short and standard acquisitions

Based on the analysis of noise level described below, we selected three reconstructions for which the noise was not statistically different, compared to the standard reconstruction ($2i10sPSF90_{sec}$): $1i10s20_{sec}$, $1i10s30_{sec}$, and $2i10sPSF60_{sec}$, which were randomly assigned to 4 PET readers with at least a 12-month experience in the reading of PET images using the Vereos system. A fifth reader was asked to read all these reconstructions as well as the standard reconstruction, starting with the supposedly worst reconstruction (in terms of noise level) and increasing the time per bed position up to the standard acquisition time. The order of review was (1) $1i10s10_{sec}$, (2) $1i10s20_{sec}$, (3) $1i10s30_{sec}$, (4) $2i10sPSF60_{sec}$ and finally the standard of reference $2i10sPSF90_{sec}$.

PET readers rated the image quality according to a 3-point scale (1=poor; 2=fair; 3= good), recorded the number of malignant foci (0, 1, 2-5, >5) and the number of anatomical sites (0, 1, 2, 3, 4, ≥5). The 5 cutoff value was chosen as this figure is commonly used by the oncology community to define oligometastic disease. We also focused on the number of anatomical sites, which is even more important than the number of lesions by organ in the staging system of many cancer types. Readers were aware of the reasons why the patients had been referred to an ^{18}F-FDG PET examination, in order to avoid bias in interpretations.

Statistical analysis

Quantitative data are presented as mean ± standard deviation (SD).

Noise (in the liver, aorta and psoas), lesion/background ratios and mean image quality were compared using the non-parametric rank-sum Friedmann test for multiple paired sample. For that test, the mean rank of each reconstruction was compared to the standard acquisition and reconstruction set (i.e 90s per bed, 2i20s, PSF modeling enabled), which was used as a control reconstruction. The aim was to seek reconstruction settings where the noise level was not statistically significant, compared to the standard reconstruction, which would therefore be useable in clinical practice with an acceptable loss in image quality. The reported P values were corrected for

multiple comparison testing using the Dunns' method. Inter-observer agreement was evaluated using the Cohen's Kappa. Kappa values were reported using the benchmarks of Landis and Koch (0.81–1 almost perfect agreement, 0.61–0.80 substantial agreement, 0.41–0.60 moderate agreement and 0.21–0.40 fair agreement). Graphs and statistical analysis were performed using Prism 8 (Graphpad, graphpad Software, San Diego, CA, USA) and XLSTAT (addinsoft, Paris France).

Results

Comparison of short and standard acquisitions: noise level, contrast and visual image quality

Over a nine-month period, twenty-eight patients were included. During this period, 873 patients were referred for ^{18}F-FDG PET. Therefore, the prevalence of patients potentially requiring fast PET imaging was 3.4%. Their characteristics are displayed on Table 1.

Noise level, expressed as the coefficient of variation (CoV) in the blood pool (aorta), liver and muscle was 0.12 (0.04), 0.12 (0.04) and 0.17 (0.08), respectively for the standard reconstruction ($2i10sPSF90_{sec}$) (Figure 2). If the same reconstruction parameters were maintained (2 iterations, 10 subsets and PSF modeling), only the 60s per bed reconstruction displayed a noise level comparable to the standard reconstruction, with $CoV\text{-}_{AORTA,}$ $CoV\text{-}_{LIVER}$ and $CoV\text{-}_{MUSCLE}$ of 0.14 (0.04), 0.15 (0.04) and 0.20 (0.09), respectively. For reconstruction with a shorter time per bed, maintaining a noise level not significantly higher than that of the standard reconstruction required disabling PSF and decreasing the number of iterations by a two-fold factor in images with less than 60s per bed position. Using these parameters, the 30s ($1i10s30_{sec}$) and 20s ($1i10s20_{sec}$) per bed reconstructions displayed $CoV\text{-}_{AORTA,}$ $CoV\text{-}_{LIVER}$ and $CoV\text{-}_{MUSCLE}$ of 0.11 (0.03), 0.12 (0.03) and 0.14 (0.05) and 0.13 (0.04), 0.14 (0.03) and 0.17 (0.07), respectively. Despite adaptation of the reconstruction parameters, the shortest reconstruction used (10s per bed) showed a significantly higher noise, compared to the standard clinical reconstruction (Figure 2).

Based on this analysis of noise level, we selected three reconstructions for comparison of lesion to background ratios and visual image quality: $1i10s20_{sec}$, $1i10s30_{sec}$, and $2i10sPSF60_{sec}$ (Figure 4). Only the 60s per bed reconstruction displayed a mean lesion/background ratio comparable to the standard reconstruction: 3.19 (1.51) versus 3.22 (1.57). For the 30s and 20s time per bed reconstructions, mean lesion/background ratios for the most obvious lesion were still both higher than 2.0 {2.43 (0.93) and 2.43 (0.91)} but represented a decrease of 22% and 23%, respectively

compared to the standard reconstruction (Figure 3a). For the less obvious lesion, mean lesion/background ratios were almost similar to those obtained with the most obvious lesion {1.99 (0.54) and 2.01 (0.56)} and represented a decrease of 21% and 22%, respectively compared to the standard reconstruction (Figure 3b). Concerning mean quality scores, the only reconstruction displaying no significant difference as compared to the standard reconstruction is the $1i10s30_{sec}$ reconstruction. It showed a mean quality score equal to 2.6 (0.5) versus 2.7 (0.5) for the standard reconstruction. All other reconstructions showed significantly slightly lower mean quality scores (Figure 4a).

Impact of acquisition time on Lesion detectability

Intra observer agreement

As described in the *Material and Methods* section, intra rater agreement was evaluated by a PET reader who interpreted all reconstructions, starting with the supposedly worst reconstruction (in terms of noise level) and increasing the time per bed position up to the standard acquisition time. The best intra rater agreements were observed with the 2i10sPSF60s for both the number of detected lesions and the number of detected anatomical sites. Regarding the number of detected lesions, the Cohen kappa coefficients were equal to 0.78, 0.72 and 0.89 for $1i10s20_{sec}$, $1i10s30_{sec}$, and $2i10sPSF60_{sec}$, respectively. For the number of detected anatomical sites, the Cohen kappa coefficients were equal to 0.72, 0.72 and 0.95 for $1i10s20_{sec}$, $1i10s30_{sec}$, and $2i10sPSF60_{sec}$, respectively. However, all Cohen kappa coefficients were ranged at least good, whatever the reconstruction used.

Regarding the number of detected lesions, 3 (11%) patients had fewer lesions detected using the $1i10s20_{sec}$, $1i10s30_{sec}$ reconstructions as compared to the $2i10sPSF60_{sec}$ and/or the standard reconstruction (Figure 4b). In line with those findings, 6 (22%) had fewer anatomical sites detected with the $1i10s20_{sec}$, $1i10s30_{sec}$ reconstructions (Figure 4c). Representative images of one of these

patients are displayed on Figure 5. Of note, in line with noise level evaluation (Figure 1), no false positive findings related to noise level were observed on the 1i10s20$_{sec}$ and 1i10s30$_{sec}$ reconstructions.

Inter observer agreement

As described in the *Material and Methods* section, the three selected reconstructions (1i10s20$_{sec}$, 1i10s30$_{sec}$, and 2i10sPSF60$_{sec}$) were randomly assigned to 3 other PET readers. Inter-rater agreement for the number of involved anatomical sites and detected lesion was good or almost perfect (Kappa: 0.64-0.91) for all the selected acquisitions (Table 2). In particular, kappa coefficients for the 30s per bed acquisition were 0.79 and 0.91 for lesion and anatomical sites number, respectively. Regarding the number of detected lesions, discordances occurred in 6, 4 and 4 patients for 1i10s20sec, 1i10s30sec, and 2i10sPSF60sec reconstructions, respectively. Regarding the number of detected anatomical sites, discordances occurred in 7, 2 and 4 patients for 1i10s20$_{sec}$, 1i10s30$_{sec}$, and 2i10sPSF60$_{sec}$ reconstructions, respectively.

Discussion

For a PET centre, being able to perform fast imaging may be a challenge, as shown in Figure. 6 where a lymphoma patient with a bulky mediastinal mass and a superior vena cava syndrome had to be scanned with several pillows to cope with dyspnea. This study was conducted as a non-inferiority study to seek the fastest acquisition time possible with our system, focusing on a specific population likely to benefit from fast or ultra-fast imaging: patients in pain, experiencing dyspnea and pediatric patients. Claustrophobic patients were not included but could also benefit from fast imaging.

This type of study could be applied to modern PET scanners capable of high-count rate. Hence, a recent evaluation of the Vereos system showed that its NECR is 513.4 Kcps @ 54.9 KBq/cc [5]. This can be compared to a NECR of 185 Kcps @ 29 KBq/cc and 266.3 Kcps @ 20.8 KBq/cc for the Siemens mCT [9] and the GE Discovery MI (5 ring version) [4], respectively.

The liver, which is the organ of reference in many circumstances (Deauville score, and marker of quality for PERCIST, where absolute and relative variation in liver uptake have to remain below 0.3 units and 20%, respectively [10]) was used, together with the vascular background in the aorta and muscle. Concordant results were obtained when comparing the level of noise in these three reference organs amongst simulated short acquisitions, provided that the shortest acquisitions were improved by decreasing the number of iterations and disabling PSF modeling. TOF was enabled for all reconstructions, as it has been shown that the improved TOF capabilities of modern digital PET systems leads to a dramatically enhanced image quality, as compared with analog PET, which may prove particularly useful for PET exams performed with reduced injected activities and/or recording times [11].

Based on noise in reference organs, we studied intra- and inter-observer analysis amongst the reconstructions deemed to be best suitable for fast imaging, i.e 1i10s20$_{sec}$, 1i10s30$_{sec}$, and

2i10sPSF60$_{sec}$. The 30s per bed position reconstruction appeared to be suitable for clinical practice, with intra observer agreement of 0.79 and 0.90 for lesion and anatomical sites number and a mean image quality comparable to that of the standard reconstruction (2.6 +/- 0.5 versus 2.7 +/- 0.5, P ns).

Of note, while we focused on adapted reconstructions displaying a noise level comparable to a standard reconstruction, one could decide to perform ultra-fast PET acquisitions despite an increase in noise level. As shown in Figure 1, an acquisition with 10 s per bed position would visually lead to a significant level of noise in the liver but still allows visualization of the tumour. This increase in noise level in an organ frequently used as a reference (for example for PERCIST [12], Deauville scoring [13]) and being part of the metastatic spread of many cancer types [14] was 73% on average when comparing the 1i10s10$_{sec}$ and 1i10s30$_{sec}$ reconstructions (Figure 2).

The relatively small number of patients included in this study could be regarded as a limitation of it, but in fact reflects the prevalence of patients potentially requiring fast PET imaging (3.4%) at our institution. This figure is related to the population scanned, in our case 90% of the PET scans performed in our department are oncology-related [15]. Secondly, we arbitrarily decided to increase the injected activity. One might assume that a clinical situation requiring fast imaging may occur after the ^{18}F-FDG has been injected. Data regarding this situation are provided as supplementary file and show similar results for noise level but tumour to background ratio smaller than 2 for the less obvious lesions, requiring further studies before being applied.

Our data could be useful to other centers facing the situation of patients experiencing pain, dyspnea or any other disease requiring a decreased acquisition time. In our experience, from a practical point of view, fast scanning requires a sufficient number of technologists and physicians to position the patient on the table of the PET scanner and remove him/her promptly and efficiently (with the appropriate equipment in the case of bedridden patients) so that the time spared during acquisition (and the gain in patient' comfort) is not lost during these phases. Median estimated total PET acquisition time for the 1i10s30$_{sec}$ was 4 min, compared to 12 min for the standard reconstruction.

It is noteworthy that PET systems with very long axial field-of-view such as total body PET [16, 17] would obviously allow ultra-fast imaging but this new technology is unlikely to be widely available given its cost. Perspectives of fast PET imaging using modern PET systems will require adaptation of the reconstruction parameters for a given system, and are likely to be impacted by evolution of reconstruction capabilities, especially implementation of deep learning reconstruction [18-20], enabling handling of noise level at low-count statistics.

Conclusion

Acquisition time per bed on the Vereos system can be reduced down to 30s without significant impact on quantitative and visual image quality and with preservation of a good detectability as compared to the standard reconstruction. These fast acquisitions require optimization of reconstruction parameters.

Bibliographie

[1] C.S. van der Vos, D. Koopman, S. Rijnsdorp, A.J. Arends, R. Boellaard, J.A. van Dalen, M. Lubberink, A.T.M. Willemsen, E.P. Visser, Quantification, improvement, and harmonization of small lesion detection with state-of-the-art PET, European journal of nuclear medicine and molecular imaging 44 (2017) 4-16.
[2] F. Fuentes-Ocampo, D.A. Lopez-Mora, A. Flotats, G. Paillahueque, V. Camacho, J. Duch, A. Fernandez, A. Domenech, M. Estorch, I. Carrio, Digital vs. analog PET/CT: intra-subject comparison of the SUVmax in target lesions and reference regions, European journal of nuclear medicine and molecular imaging 46 (2019) 1745-1750.
[3] D.A. Lopez-Mora, A. Flotats, F. Fuentes-Ocampo, V. Camacho, A. Fernandez, A. Ruiz, J. Duch, M. Sizova, A. Domenech, M. Estorch, I. Carrio, Comparison of image quality and lesion detection between digital and analog PET/CT, European journal of nuclear medicine and molecular imaging 46 (2019) 1383-1390.
[4] T. Pan, S.A. Einstein, S.C. Kappadath, K.S. Grogg, C. Lois Gomez, A.M. Alessio, W.C. Hunter, G. El Fakhri, P.E. Kinahan, O.R. Mawlawi, Performance evaluation of the 5-Ring GE Discovery MI PET/CT system using the national electrical manufacturers association NU 2-2012 Standard, Medical physics 46 (2019) 3025-3033.
[5] I. Rausch, A. Ruiz, I. Valverde-Pascual, J. Cal-Gonzalez, T. Beyer, I. Carrio, Performance Evaluation of the Vereos PET/CT System According to the NEMA NU2-2012 Standard, Journal of nuclear medicine : official publication, Society of Nuclear Medicine 60 (2019) 561-567.
[6] J. van Sluis, R. Boellaard, A. Somasundaram, P. van Snick, R. Borra, R. Dierckx, G. Stormezand, A. Glaudemans, W. Noordzij, Image quality and semi-quantitative measurements of the Siemens Biograph Vision PET/CT: Initial experiences and comparison with Siemens Biograph mCT PET/CT, Journal of nuclear medicine : official publication, Society of Nuclear Medicine (2019).
[7] A. Aljared, A.A. Alharbi, M.W. Huellner, BSREM Reconstruction for Improved Detection of In-Transit Metastases With Digital FDG-PET/CT in Patients With Malignant Melanoma, Clinical nuclear medicine 43 (2018) 370-371.
[8] J. Salvadori, L. Imbert, M. Perrin, G. Karcher, Z. Lamiral, P.Y. Marie, A. Verger, Head-to-head comparison of image quality between brain (18)F-FDG images recorded with a fully digital versus a last-generation analog PET camera, EJNMMI research 9 (2019) 61.
[9] I. Rausch, J. Cal-Gonzalez, D. Dapra, H.J. Gallowitsch, P. Lind, T. Beyer, G. Minear, Performance evaluation of the Biograph mCT Flow PET/CT system according to the NEMA NU2-2012 standard, EJNMMI physics 2 (2015) 26.
[10] R.L. Wahl, H. Jacene, Y. Kasamon, M.A. Lodge, From RECIST to PERCIST: Evolving Considerations for PET response criteria in solid tumors, Journal of nuclear medicine : official publication, Society of Nuclear Medicine 50 Suppl 1 (2009) 122S-50S.
[11] J. Salvadori, F. Odille, A. Verger, P. Olivier, G. Karcher, P.Y. Marie, L. Imbert, Head-to-head comparison between digital and analog PET of human and phantom images when optimized for maximizing the signal-to-noise ratio from small lesions, EJNMMI physics 7 (2020) 11.
[12] K. Pinker, C. Riedl, W.A. Weber, Evaluating tumor response with FDG PET: updates on PERCIST, comparison with EORTC criteria and clues to future developments, European journal of nuclear medicine and molecular imaging 44 (2017) 55-66.
[13] C. Nanni, A.S. Cottereau, E. Lopci, C. Bodet-Milin, M. Coronado, B. Pro, W.S. Kim, J. Trotman, S. Barrington, U. Duhrsen, T. Vander Borght, E. Zamagni, F. Kraeber-Bodere, C. Messiou, A. Rahmouni, I. Buvat, M. Andre, M. Hertzberg, W. Oyen, O. Casasnovas, S. Luminari, L. Garderet, F. Montravers, C. Kobe, R. Kluge, A. Versari, E. Zucca, P. Moreau, B. Cheson, C. Haioun, A. Gallamini, M. Meignan, Report of the 6th International Workshop on PET in lymphoma, Leuk Lymphoma 58 (2017) 2298-2303.
[14] E. Viadana, I.D. Bross, J.W. Pickren, The metastatic spread of cancers of the digestive system in man, Oncology 35 (1978) 114-26.
[15] C. Lasnon, B. Houdu, E. Kammerer, T. Salomon, J. Devreese, A. Lebasnier, N. Aide, Patient's weight: a neglected cause of variability in SUV measurements? A survey from an EARL accredited

PET centre in 513 patients, European journal of nuclear medicine and molecular imaging 43 (2016) 197-199.
[16] S.R. Cherry, T. Jones, J.S. Karp, J. Qi, W.W. Moses, R.D. Badawi, Total-Body PET: Maximizing Sensitivity to Create New Opportunities for Clinical Research and Patient Care, Journal of nuclear medicine : official publication, Society of Nuclear Medicine 59 (2018) 3-12.
[17] R.D. Badawi, H. Shi, P. Hu, S. Chen, T. Xu, P.M. Price, Y. Ding, B.A. Spencer, L. Nardo, W. Liu, J. Bao, T. Jones, H. Li, S.R. Cherry, First Human Imaging Studies with the EXPLORER Total-Body PET Scanner, Journal of nuclear medicine : official publication, Society of Nuclear Medicine 60 (2019) 299-303.
[18] J. Cui, K. Gong, N. Guo, C. Wu, X. Meng, K. Kim, K. Zheng, Z. Wu, L. Fu, B. Xu, Z. Zhu, J. Tian, H. Liu, Q. Li, PET image denoising using unsupervised deep learning, European journal of nuclear medicine and molecular imaging (2019).
[19] W. Lu, J.A. Onofrey, Y. Lu, L. Shi, T. Ma, Y. Liu, C. Liu, An investigation of quantitative accuracy for deep learning based denoising in oncological PET, Physics in medicine and biology 64 (2019) 165019.
[20] G. Wang, J.C. Ye, K. Mueller, J.A. Fessler, Image Reconstruction is a New Frontier of Machine Learning, IEEE transactions on medical imaging 37 (2018) 1289-1296

« Par délibération de son Conseil en date du 10 Novembre 1972, l'Université n'entend donner aucune approbation ni improbation aux opinions émises dans les thèses ou mémoires. Ces opinions doivent être considérées comme propres à leurs auteurs ».

VU, le Président de Thèse

VU, le Doyen de la Faculté

VU et permis d'imprimer
en référence à la délibération
du Conseil d'Université
en date du 14 Décembre 1973

Pour le Président
de l'Université de CAEN et P.O

Le Doyen

ANNEE DE SOUTENANCE : 2020

NOM ET PRENOM DE L'AUTEUR : COUDRAIS NICOLAS

TITRE DE LA THESE: À quelle vitesse pouvons-nous scanner des patients avec des systèmes TEP/TDM modernes (numériques) ?

RESUME DE LA THESE EN FRANÇAIS :

Objectif:
Rechercher la durée minimale d'acquisition avec un système TEP numérique sans compromettre la qualité d'image et la détection des lésions chez les patients nécessitant une imagerie rapide TEP 18F-FDG.

Matériels et méthodes:
28 patients ont été scannés sur un système TEP numérique Vereos. Les données ont été reconstruites avec un laps de temps décroissant jusqu'à 10 secondes par position de lit. Le bruit a été évalué en utilisant des ratios cible/bruit de fond, dans le foie, les vaisseaux et les muscles. 5 médecins ont enregistré la qualité d'image, le nombre de foyers et de sites anatomiques impliqués dans des reconstructions allant de 60 à 10sec par pas, par rapport à la reconstruction standard de 90sec.

Résultats:
Les reconstructions suivantes, avec un bruit non significativement supérieur à la reconstruction standard, ont été sélectionnées: 1itération/10 sous-ensembles/20sec (1i10s20sec), 1i10s30sec et 2i10sPSF60sec.
Seuls les 60sec par pas avaient des ratios cible/arrière-plan similaires à ceux de la reconstruction standard, mais les ratios moyens étaient toujours supérieurs à 2,0 pour la reconstruction des 30. L'accord inter-évaluateur et intra-évaluateur pour le nombre de sites anatomiques et de lésions détectées était bon voir presque parfait, en particulier pour les acquisitions de 30sec. Le temps d'acquisition total estimé de TEP pour le 1i10s30sec et la reconstruction standard étaient respectivement de 4 et 12 min.

Conclusion:
L'imagerie rapide est possible avec des acquisitions de 30sec par position de lit sur le système Vereos, nécessitant une optimisation des paramètres de reconstruction.

MOTS CLES : TEP; Numérique; ^{18}F-FDG; douleur; dyspnée

ANNEE DE SOUTENANCE : 2020

NOM ET PRENOM DE L'AUTEUR : COUDRAIS NICOLAS

TITRE DE LA THESE EN ANGLAIS: How fast can we scan patients with modern (digital) PET/CT systems?

RESUME DE LA THESE EN ANGLAIS :

Purpose:
To seek the minimal duration per bed position with a digital PET system without compromising image quality and lesion detection in patients requiring fast 18F-FDG PET imaging.

Materials and methods:
28 patients were scanned on a Vereos system. List mode data were reconstructed with decreasing time frame down to 10s per bed position. Noise was evaluated in the liver, blood pool and muscle, and using target-to-background ratios. 5 PET readers recorded image quality, number of clinically relevant foci and of involved anatomical sites in reconstructions ranging from 60 to 10s per bed position, compared to the standard 90s reconstruction.

Results:
The following reconstructions, which harboured a noise not significantly higher than the standard reconstruction, were selected: 1iteration/10subsets/20sec (1i10s20sec), 1i10s30sec, and 2i10sPSF60sec.
Only the 60s per bed displayed similar target-to-background ratios compared to the standard reconstruction, but mean ratios were still higher than 2.0 for the 30s reconstruction. Inter-rater agreement for the number of involved anatomical sites and detected lesion was good or almost perfect (Kappa: 0.64-0.91). In particular, kappa for the 30s per bed acquisition was 0.78 and 0.91 for lesion and anatomical sites number, respectively. Intra-rater agreement was also excellent for the 30s reconstruction. Estimated total PET acquisition time for the 1i10s30sec, and the standard reconstruction were 4 and 12 min, respectively.

Conclusion:
Fast imaging is feasible with state-of-the-art PET systems. Acquisitions of 30s per bed position are feasible with the Vereos system, requiring optimization of reconstruction parameters.

KEY WORDS: PET; Digital; ^{18}F-FDG; pain; dyspnea